Journal of Cell Science 112, 3463-3475 (1999)
Printed in Great Britain © The Company of Biologists Limited 1999
JCS0386

Dynamics of the nuclear lamina as monitored by GFP-tagged A-type lamins

Jos L. V. Broers[1,*], Barbie M. Machiels[1], Guillaume J. J. M. van Eys[1], Helma J. H. Kuijpers[1], Erik M. M. Manders[1], Roel van Driel[2] and Frans C. S. Ramaekers[1]

[1]Department of Molecular Cell Biology and Genetics, University of Maastricht, PO Box 616, 6200 MD Maastricht, The Netherlands
[2]E. C. Slater Instituut, Biocentrum Amsterdam, University of Amsterdam, The Netherlands
*Author for correspondence (e-mail: Jos.Broers@molcelb.unimaas.nl)

Accepted 2 July; published on WWW 30 September 1999

SUMMARY

The behavior of chimeric proteins consisting of A-type lamins and green fluorescent protein (GFP) was studied to investigate the localization and dynamics of nuclear lamins in living cells. Cell line CHO-K1 was transfected with cDNA constructs encoding fusion proteins of lamin A-GFP, lamin AΔ10-GFP, or lamin C-GFP. In the interphase nucleus lamin-GFP fluorescence showed a perinuclear localization and incorporation into the lamina for all three constructs. Our findings show for the first time that the newly discovered lamin AΔ10 protein is localized to the nuclear membrane. The GFP-tagged lamins were processed and behaved similarly to the endogenous lamin molecules, at least in cells that expressed physiological levels of the GFP-lamins. In addition to the typical perinuclear localization, in the majority of transfected cells each individual A-type lamin-GFP revealed an extensive collection of branching intra- and trans-nuclear tubular structures, which showed a clear preference for a vertical orientation. Time-lapse studies of 3-D reconstructed interphase cells showed a remarkable stability in both number and location of these structures over time, while the lamina showed considerable dynamic movements, consisting of folding and indentation of large parts of the lamina. Fluorescence recovery after bleaching studies revealed a low protein turnover of both tubular and lamina-associated lamins. Repetitive bleaching of intranuclear areas revealed the presence of an insoluble intranuclear fraction of A-type lamins. Time-lapse studies of mitotic cells showed that reformation of the lamina and the tubular structures consisting of A-type lamins did not occur until after cytokinesis was completed.

Key words: Lamin, Green fluorescent protein, Vital imaging, Nuclear matrix, Mitosis

INTRODUCTION

Lamins are the major constituents of the nuclear lamina. Two main types of lamins, A-type lamins and B-type lamins, can be distinguished. While B-type lamins are encoded by distinct genes (Biamonti et al., 1992; Pollard et al., 1990), A-type lamins (lamins A and lamin C) arise from a single gene by alternative splicing (Furakawa et al., 1994; Lin and Worman, 1993; Machiels et al., 1996). Recently, we described a new splicing product of the lamin A/C gene, which is identical to lamin A except that exon 10 is missing. The new protein was therefore designated lamin AΔ10. The presence of lamin AΔ10 mRNA has been demonstrated in many cell lines and human tissues (Machiels et al., 1996). Since lamin AΔ10 is largely identical to lamin A, generation of antibodies specifically directed against this new protein proved to be unsuccessful. Consequently, the cellular localization of lamin AΔ10 could not be established by immunocytochemistry.

In addition to their presence in the nuclear lamina, both A- and B-type lamins form intranuclear structures (Bridger et al., 1993; Moir et al., 1994) and even transnuclear tube-like structures (Fricker et al., 1997). However, it is not known whether these tubular structures contain all three A-type lamin subtypes. A-type lamin expression is dependent on the degree and type of differentiation, as well as the proliferative status of cells and tissues. For instance, A-type lamins are virtually absent from most embryonic cells (Gerace and Burke, 1988; Krohne and Benavente, 1986; Nigg, 1992; Riemer et al., 1995; Röber et al., 1989), the proliferative compartment of several epithelia (Broers et al., 1997) and spermatogonia (Machiels et al., 1997), and present in most well-differentiated cell-types (Broers et al., 1997; Cance et al., 1992).

Although several studies speculate about the function of nuclear lamins, the role of the different lamins in processes such as cell cycle progression, nuclear chromatin organization and regulation of transcription is still unclear. Recent studies showed that lamina flexibility is required for growth of the nuclear envelope and for nuclear volume increase during the cell cycle. Progression into S-phase is dependent on the acquisition of a minimal nuclear volume (Yang et al., 1997b). Moreover, disruption of the nuclear lamina after microinjection of truncated lamin A inhibits DNA synthesis (Spann et al., 1997). Similar experiments in cells transfected with Xlamin B1 deletion constructs did not, however, result in disruption of the replication centers (Ellis et al., 1997).

A major drawback in studying nuclear lamin function until now has been the inability to examine individual lamins in living cells for extended periods of time. Green fluorescent

protein (GFP)-tagged lamins offer this possibility. GFP and its mutants (Cubitt et al., 1995; Heim et al., 1995) have been used as reporter proteins in bacteria (Chalfie et al., 1994), yeast (Monosov et al., 1996), plants (Chiu et al., 1996) and mammalian cells (Cheng et al., 1996; Yeh et al., 1995). GFP requires no substrates, cofactors or other proteins to fluoresce (Chalfie et al., 1994) and is a relatively small protein (27 kDa). Chimeric proteins of GFP with several distinct target proteins have shown their usefulness for localization and trafficking studies in a variety of living cells (De Giorgi et al., 1996; Ludin et al., 1996; Marshall et al., 1995; Ogawa et al., 1995; Olson et al., 1995; Rizzuto et al., 1995). In this study we have used chimeric GFP constructs of all three A-type lamins to visualize their dynamics in living cells, and to monitor the behaviour of these nuclear constituents independently of each other, circumventing possible artifacts that could be introduced by fixation of the cells.

MATERIALS AND METHODS

Plasmids

Lamin A-cDNA, kindly provided by Dr F. McKeon (McKeon et al., 1986), was ligated to the 3′ end of GFP in the mammalian expression vector pS65T-C1 (Clontech Laboratories Inc., Palo Alto, CA, USA) using the *Sst*II and *Bam*HI sites, generating pS65T-lamA. Lamin AΔ10-cDNA (Machiels et al., 1996) was ligated into pS65T-C1 using the *Sst*II and *Bam*HI sites, generating pS65T-lamAΔ10.

pS65T-lamC was generated by replacement of the 3′ *Bsi*WI/*Bam*HI fragment of pS65T-lamA, encoding part of exon 9 and exons 10, 11 and 12 of lamin A, by the 3′ end of lamin C. The 3′ end of lamin C was obtained by RT-PCR (Machiels et al., 1996). In the first round of PCR, primer A22 (sense, 5′-GCCTACCGCAAGCTCTTGGA-3′, corresponding to nucleotides 1123-1142 of lamins A and C; Eurogentec, Seraing, Belgium) and primer X37 (antisense, 5′-TGAAAAGATTTTTGGCACGG-3′, corresponding to nucleotides 1798-1779 of the untranslated region of lamin C; Eurogentec) were used, followed by a second round of PCR with nested primer Apr1 (sense, 5′-AGCCTGCGTACGGCTCTCAT-3′; *Bsi*WI site underlined; corresponding to nucleotides 1573-1592 of lamins A and C; Eurogentec) and primer Bar30 (antisense, 5′-TATAGGATCCC-GGCCTCAGCGGCGGCTACC-3′; *Bam*HI site underlined; the 20 3′ bases are complementary to nucleotides 1724-1705 of lamin C, the 10 5′ bases are non-complementary, but contain a *Bam*HI site for cloning; Gibco Life Technologies Ltd., Paisley, Scotland). The *Bsi*WI and *Bam*HI sites were used for cloning of the 3′ lamin C PCR product into pS65T-lamA, resulting in pS65T-lamC.

Cell culture and transfections

CHO cells were grown on HAM's F12 medium (ICN Biomedicals Inc., Costa Mesa, CA, USA) supplemented with 10% fetal calf serum (FCS, Gibco Life Technologies Ltd.) and 2 mM L-glutamine. Cell cultures were maintained in an incubator with 5% CO_2 at 37°C. For transfections, cells were grown to 25-30% confluency in 6-well plates. A mixture of 2.5 μg plasmid DNA, 20 mM Hepes and DOTAP (Boehringer Mannheim GmbH, Mannheim, Germany) was added to 2.5 ml culture medium, according to the manufacturer's instructions. The cells were grown overnight in the DOTAP/DNA-containing culture medium. The medium was then replaced by culture medium without DOTAP/DNA, and geneticin (G418, Gibco Life Technologies Ltd) was added after 6 hours to a final concentration of 500 μg/ml. Stable transfectants were subcloned and grown in culture medium without geneticin. To enhance fluorescence cells were grown at 30°C for up to 3 days prior to further handling.

Blocking of farnesylation was achieved by the addition of 50 μM lovastatin, kindly provided by Merck (Rahway, NJ, USA). Cells were cultured overnight in the presence of lovastatin, and fixed with methanol and acetone (see below) for immunocytochemistry.

Antibodies

The following mouse monoclonal antibodies were used in this study. 41CC4 (IgM), which recognizes lamins A and C and does not react with human B-type lamins, was used as undiluted culture supernatant (Burke et al., 1983). R27 (IgM), which recognizes lamins A and C, was used as undiluted culture supernatant in immunoblotting (Zatloukal et al., 1992). 133A2 (IgG3) was a kind gift of Dr Y. Raymond (Montréal, Canada). It was raised against the carboxy terminus of 98 amino acids present in lamin A and absent from lamin C. This antibody recognizes lamin A, reacting with the epitope consisting of amino acids 598-611 (Hozák et al., 1995). Antibody 133A2 was used as 1:2500 diluted mouse ascites in immunofluorescence. PC10, which recognizes the proliferating cell nuclear antigen (PCNA), used at a dilution of 1:100, was kindly provided by Dr David Lane (Dundee, UK).

The following polyclonal rabbit antibodies were used. Antibody α-PA, raised against the 15 amino acids of prelamin A, which are proteolytically removed during the farnesylation-dependent processing of this molecule (Sinensky et al., 1994a). This antibody was used at a dilution of 1:200. An antibody directed against GFP (Clontech Laboratories, Palo Alto, CA, USA) was used at a dilution of 1:5000 in immunofluorescence studies.

Indirect immunofluorescence technique

The indirect immunofluorescence assay was applied to cell cultures that were grown on coverslips for up to 3 days at 30°C. After washing in phosphate-buffered saline (PBS, containing 8 g/l NaCl, 0.2 g/l KCl, 1.15 g/l Na_2HPO_4 and 0.2 g/l KH_2PO_4 at pH 7.4) the cells were either immediately fixed, or first detergent-extracted (see below) and than fixed using methanol (–20°C for 5 seconds), followed by acetone (4°C, 3 times for 5 seconds) and air dried. Alternatively, cells were fixed in 3.7% formaldehyde in PBS for 15 minutes at room temperature room temperature (RT) followed by permeabilization using 0.1% Triton X-100 (BDH, Poole, UK) in PBS for 10 minutes at RT. Cells were then incubated with the primary antibody for 30-45 minutes at RT, and after several washes with PBS, incubated for 30-45 minutes with Texas Red-conjugated goat anti-mouse Ig (diluted 1:80, Southern Biotechnology Associates; SBA/ITK; Birmingham, AL, USA), with Texas Red-conjugated goat anti-mouse IgM (diluted 1:80, SBA/ITK), or with Texas Red-conjugated goat anti-rabbit Ig (diluted 1:80, SBA/ITK). Thereafter, cells were washed in PBS, mounted in 90% glycerol containing 0.02 M Tris-HCl pH 8.0, 0.002% NaN_3, 2% 1,4 diazabicyclo (2,2,2)-octane (DABCO; Merck, Darmstadt, Germany) and 0.5 μg/ml 4′,6 diamino-2 phenylindole (DAPI; Merck) or 1 μg/ml propidium iodide (Calbiochem, La Jolla, CA) and 0.1 mg/ml RNAse (Serva, Heidelberg, Germany) for DNA staining.

Conventional immunofluorescence micrographs were taken with an automatic camera using Kodak 400 ASA Tri-X pan film. Alternatively, confocal images were generated (see below).

Membrane staining

Membrane staining was performed with rhodamine B hexyl ester dye (R6; Molecular Probes, Eugene, OR) in a concentration of 0.5 μg/ml culture medium for 5 minutes at 37°C. The cells were then washed with PBS and fixed for 15 minutes at RT using 3.7% formaldehyde buffered with PBS. After a PBS wash the cells were mounted with glycerol/PBS (1:1 v/v).

Preparations of cytoskeletal fractions and of in situ nuclear matrices

Cytoskeletal cell preparations were made as described previously (Machiels et al., 1995). In brief, cells were harvested by scraping and

extracted using 0.5% Triton X-100 (BDH, Poole, England) for 10 minutes at 0°C, followed by treatment with 1 mg/ml DNAse 1 (Sigma) and 50 μg/ml RNAse A (Sigma) for 20 minutes at RT. Finally the pellet was resuspended in SDS-sample buffer (Laemmli, 1970) and boiled for 5 minutes.

Nuclear matrix preparations of cultured cells were prepared as described before (Verheijen et al., 1989). In brief, cells grown on coverslips were extracted for 10 minutes at 0°C with a buffer containing 5 mM N-ethylmaleimide (NEM, Sigma, St Louis, MO, USA), 0.5% Triton X-100 and appropriate protease inhibitors, followed by extraction in a buffer containing 0.5% sodium deoxycholate (DOC; Merck) and 1% Tween 40 (Sigma). Cell remnants were incubated in a buffer containing 1 mg/ml DNAse 1 (Sigma) and 50 μg/ml RNAse A (Sigma), and finally extracted with a high-salt buffer containing 400 mM $(NH_4)_2SO_4$, 50 mM Tris-acetate, 1.5 mM $MgCl_2$, 0.5 mM PMSC and 5 mM NEM for 10 minutes at 0°C.

Vital imaging and image restoration

For visualization of lamins in actively proliferating cells, cells were grown on round coverslips with a diameter of 20 mm at 30°C overnight up to 3 days and transferred to 37°C for 2-3 hours. Slides with round wells of 16-18 mm diameter and 0.6-0.8 mm depth were used to mount coverslips. Wells were first filled with 100 μl medium containing 20 mM Hepes. After face-down mounting of the coverslips excessive medium was aspired and coverslips were sealed with nail polish, ensuring that nail polish could not get into contact with culture medium. Slides were placed on a confocal microscope table heated with a fan to maintain an ambient temperature of 33-37°C. Using this system cells remained viable and actively proliferating for several hours. To prevent possible culture artifacts all recordings were performed within 3 hours after mounting of cells onto the slides.

Confocal images were collected using the BioRad MRC600 confocal scanning laser microscope (BioRad, Hempel Hempstead, UK), equipped with an air-cooled Argon-Krypton mixed gas laser and mounted onto an Axiophote microscope (Zeiss), using oil-immersion objectives (40×, NA=3D1.3 or 63×, NA=3D1.4). The laser scanning microscope was used in the dual parameter set-up, according to the manufacturer's specifications, using dual wavelength excitation at 488 nm and 568 nm. Emission spectra were separated by the standard sets of dichroic mirrors and barrier filters. Optical sections were recorded in the Kalman filtering mode using 4-8 scans for each picture. For living cells time lapse series were created by scanning at regular intervals (30-60 seconds) at a single confocal level fixed at the centre of nuclei of interest. In the case of dividing cells the focus level was adjusted synchronously with the stretching of cells.

Z-series were generated by collecting a stack consisting of 20-30 optical sections using a step size of 0.36 μm in the *z*-direction. Stacks of images were used for side-by-side stereo projection applying a pixel shift of –0.6 to –0.9 pixels between frames for the left projection and 0.6 to 0.9 pixels for the right projection, depending on the depth of the image and the number of slices of each stack, using Confocal Assistance software (BioRad). If appropriate, intensities of projected images were enhanced using Adobe Photoshop 5.0® software.

Time series of three-dimensional (3-D) stacks of living cells were recorded using a Zeiss LSM 510 confocal microscope on a Axiovert 100 microscope (Zeiss) with a planneofluar objective (100×, NA=3D1.3). Excitation was achieved with an Argon-ion laser at 488 nm. Emission was registered using a 510 LP filter. The high sensitivity of the fluorescence detection system allowed the use of extremely low laser intensities (0.3% of 15 mW maximum), reducing both phototoxic effects on cells and bleaching of the GFP signal. Each stack was made up of 16 slices (*z*-step=0.8 μm), resulting in 512×512×26 voxel images.

Alternatively, stacks were recorded using a Leica confocal laser scanning microscope, equipped with a dual wavelength (488/514 nm) argon ion laser and oil-immersion objective (100×, NA=3D1.32, *z*-step 0.2 μm). Emitted fluorescence was detected using a 525DF10 bandpass filter for FITC. 3-D images were produced as 512×512×32 voxel images. To improve the effective resolution of the confocal images and to reduce noise the Huygens System image restoration software (van der Voort and Strasters, 1995; Scientific Volume Imaging B.V., Hilversum, the Netherlands) was applied. Because of the photon-limited character of the data a Maximum Likelihood Estimation (MLE) algorithm (Shepp and Vardi, 1982) was used.

To visualise the restored images the Simulated Fluorescence Process (SFP) (van der Voort et al., 1993) algorithm of the FluVR volume-rendering software (Scientific Volume Imaging B.V.) was used. The stereoscopic pair was generated by rotating the perspective projected scene over a 2.2° angle around the origin.

Photobleaching experiments

The recovery of fluorescence after photobleaching (for a review, see Edidin, 1994) was studied using a Zeiss LSM 510 confocal microscope Bleaching experiments were electronically controlled using LSM510 software (release 2.01, Zeiss) Bleaching was achieved by performing 10 scans of a small, selected region of interest (ROI) at full laser power (0.8 mW). Recordings of the cells with a resolution of 128×128 pixels were performed before bleaching, and at 200 ms intervals after bleaching for up to 10 seconds, the average intensity of the bleached ROI was measured (at low laser power 0.008 mW). Finally, the average intensity of the ROI was monitored after 10 minutes.

In order to estimate the amount of unbound lamin-GFP molecules in intranuclear regions, the Fluorescence Loss in Photobleaching technique (Lippincott-Schwartz et al., 1999) was applied. Selected nuclear areas were repetitively bleached with 10 second intervals between each bleaching round. Each bleaching round consisted of 10 scans at full laser power (0.8 mW) of a ROI including both lamina and nucleoplasm. After each bleaching round the loss of fluorescence intensity was measured in the bleached area, and in several areas outside the bleached region, including the lamina, a nucleolar area (if visible) and an intranuclear area devoid of tubular structures (nucleoplasm).

Gel electrophoresis and immunoblotting

Protein samples were dissolved in SDS-sample buffer and one-dimensional SDS-gel electrophoresis in 10% polyacrylamide (BioRad Laboratories, Hercules, CA, USA) slab gels containing 0.1% SDS (Merck), and immunoblotting were performed as described (Machiels et al., 1995). Immunoblotting was performed using mouse monoclonal lamin antibodies as primary antibodies and peroxidase-conjugated rabbit anti-mouse Igs (1:1000) as secondary antibody (DAKO A/S, Glostrup, Denmark). Peroxidase activity was detected by chemiluminescence (ECL-kit, Amersham, Buckinghamshire, UK).

Flow cytometry

Flow cytometric analyses were performed essentially as described by Schutte et al. (1995). Untransfected CHO-K1 cells, lamin A-GFP transfected cells and lamin C-GFP transfected cells were harvested by trypsinization, fixed in cold (–20°C) methanol for 10 minutes and stained immunocytochemically using the lamin A antibody 133A2 (1:1000) and phycoerythrin (PE)-conjugated goat anti-mouse immunoglobulins (1:15, DAKO A/S, Glostrup, DK). Labelled cells were analysed using a FACSort flow cytometer and Cellquest analysis software (Becton Dickinson, Sunnyvale, CA). Excitation was done at 488 nm, and emission was detected using a 515-545 nm bandpass filter for the GFP signal and a 572-588 nm bandpass filter for the PE signal. To correct for bleed-through of the different fluorochromes, single GFP-labelled or lamin A PE-stained samples were used for calibration, resulting in compensation settings of FL1(GFP)–%FL2(PE)=4.8% and FL2–%FL1=3.1% at 537 V for FL1 and 409 V for FL2.

RESULTS

Chimeric A-type lamin-GFP proteins incorporate into the nuclear lamina

CHO-K1 cells transfected with the different A-type lamin-GFP constructs showed a stable expression of the chimeric proteins. Confocal microscopy of transfected CHO cells showed that lamin A-GFP, lamin AΔ10-GFP and lamin C-GFP were localized in the nuclear lamina of transfected cells (Fig. 1). No GFP signal in interphase cells was seen outside the nuclei, except for some isolated cytoplasmic dots. Apparently, fusion of GFP to the amino-terminal part of lamins A, AΔ10 or C does not interfere with incorporation of the fusion protein into the lamina and does not disturb lamina formation in these cells. Transfection of the GFP-cDNA construct alone showed that this protein does not specifically localize to the nucleus, but is dispersed throughout both the cytoplasm and the nucleus, and is not maintained in cells after nuclear matrix isolation procedures (not shown). Transfected chimeric proteins were recognized by the different A-type lamin antibodies (Fig. 1A,B,E) as well as the antibody to GFP (not shown). Double-fluorescence detection of lamin-GFP signal and immunostaining with antibody 133A2 to lamin A, recognizing both native lamin A and chimeric lamin A-GFP, revealed a considerable heterogeneity in lamin-GFP expression levels, which was partly reflected in the immunostaining intensities. Nuclei showing a strong GFP signal (Fig. 1A) were also brightly immunostained (Fig. 1A′). Conversely, nuclei showing a bright immunostaining (due to the presence of native lamin A) did not necessarely show a high level of lamin A-GFP expression (arrowhead in Fig. 1A,A′). At the individual cell level, colocalization of GFP-signal of lamin AΔ10-GFP and the immunofluorescence signal using the lamin A antibody at the nuclear periphery was evident (Fig. 1B,B′). This was also true for lamin A-GFP (not shown). However, the GFP signal showed more variation in intensity and many more intranuclear structures than the immunostaining (compare Fig. 1B and B′). In situ nuclear matrix isolations were performed to investigate whether all three A-type lamin-GFP proteins incorporate into the nucleus similar to native lamins. It is evident that lamin-GFP proteins are part of the nuclear matrix fraction since they were resistant to extractions with detergents, nucleases and high salt (Fig. 1C,D; see Materials and Methods). No differences in the extractability between the individual lamin-GFP proteins, or between lamin-GFP proteins and native lamins were seen (data not shown).

Immunoblotting analyses showed that stable transfected clones of CHO-K1 produced chimeric lamin A-GFP proteins of the expected sizes. In addition to protein bands corresponding to the size of native lamins A and C, detected in both untransfected and transfected cell lines, protein bands with relative mobility corresponding to molecular masses of 97 kDa (lamin A-GFP), 92 kDa (lamin AΔ10-GFP) and 87 kDa (lamin C-GFP) were seen (Fig. 1E). The amount of chimeric protein expressed as detected by immunoblotting was highly variable between different subclones (compare lanes 2 and 3).

In order to quantify expression levels of lamin-GFP versus native lamin signals, flow cytometric analyses of the fluorescence intensities were performed. Cells transfected with lamin A-GFP show a brighter immunostaining with the lamin A antibody than do untransfected cells (Fig. 2A). Note,

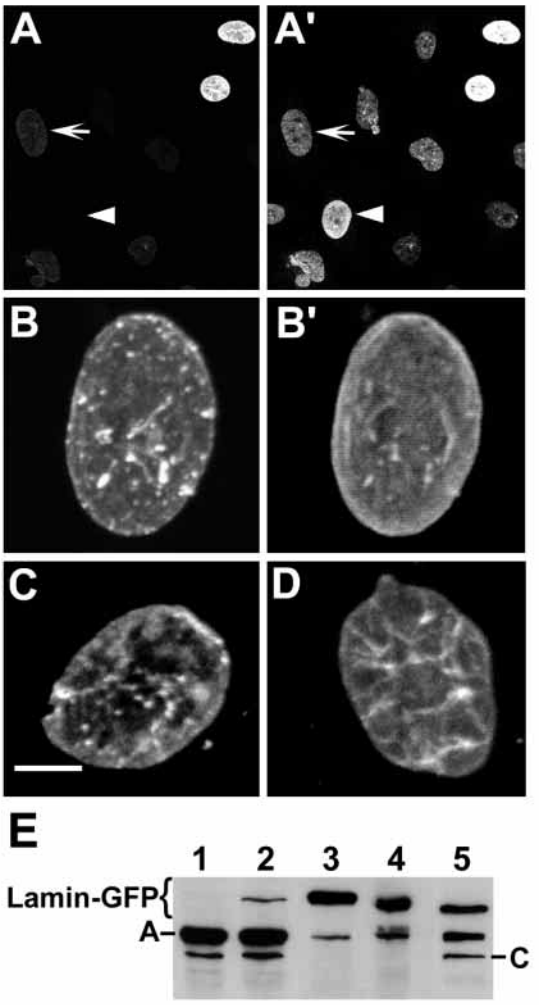

Fig. 1. (A,A′) GFP fluorescence (A) and immunostaining (A′) of a monoclonal cell culture, stably transfected with lamin A-GFP. Note the large variation in GFP signal between individual cells (A) and the only partly corresponding intensity of the lamin A-GFP immunostaining (A′). Note that nuclei showing a bright to moderately bright GFP signal (arrow) show a corresponding increased level of immunostaining. The level of lamin A-GFP expression seems to be physiological in many cells, especially since some nuclei, in which the GFP signal is barely detectable (arrowhead), can express levels of native lamins, similar to nuclei with larger amounts of lamin A-GFP. (B,B′) Linear projection of optical sections of a single nucleus of a lamin AΔ10-GFP transfected CHO-K1 cell. (B) GFP signal and (B′) immunostaining of the same nucleus. Note the prominent intranuclear structures visualized by GFP fluorescence, which are less visible with the antibody staining procedure. (C,D) Linear projection of confocal recordings of nuclear matrix preparations of lamin A-GFP (C) and lamin C-GFP (D) transfected cells. Note that lamin-GFP signals remain visible in extracted cells. (E) Immunoblotting of untransfected CHO-K1 cells (lane 1) and cells transfected with lamin A-GFP (lanes 2 and 3), lamin AΔ10-GFP (lane 4) and lamin C-GFP (lane 5), using either the lamin A antibody (lanes 1-4) or the lamin A/C antibody (lane 5). Cytoskeletal preparations were made by Triton X-100 extraction, followed by nuclease treatment of samples. Untransfected CHO cells showed a major band corresponding to lamin A (lane 1). In the transfected cell lines, in addition to the native lamin A, bands at the expected positions of the chimeric lamin A-GFP (approx. 97 kDa) and lamin AΔ10-GFP (92 kDa) are detected with the lamin A antibody (lanes 2-4). Lamin A/C antibody revealed native lamins A and C and the chimeric lamin C-GFP signal, predicted at 87 kDa (lane 5). Bar, 20 μm (A,A′), 5 μm (B-D).

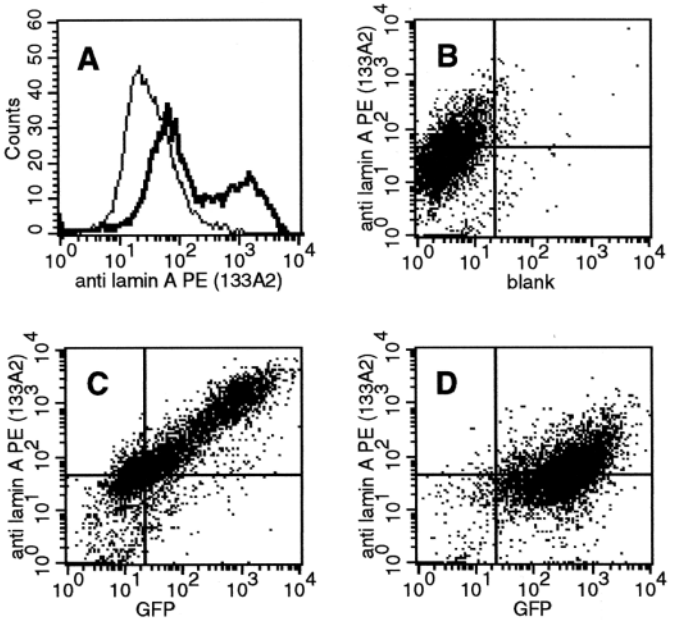

Fig. 2. Flow cytometric quantitation of relative amounts of transfected GFP-lamins. (A) Comparison of immunostaining intensities using the lamin A antibody in untransfected CHO-K1 cells (thin line), or cells transfected with lamin A-GFP (bold line). Note the variable expression of lamin A in both transfected and untransfected cells and the prominent increase of lamin A expression in only part of the lamin A-GFP transfected cells. (B) Plot histogram of a two-parameter flow cytometric analysis showing intensity of the lamin A antibody immunoreactivity versus green (auto-)fluorescence (blank) in untransfected CHO-K1 cells. (C) Two-parameter flow cytometric analysis of immunocytochemical lamin A staining versus GFP signal of lamin A-GFP transfected cells. Note the linear correlation between the intensity of lamin A antibody reactivity, and lamin A-GFP signal. (D) Two-parameter flow cytometric analysis of an immunocytochemical lamin A staining, versus GFP signal of lamin C-GFP transfected cells. Note that staining intensity as seen with the lamin A antibody is randomly correlated to the lamin C-GFP fluorescence intensity.

however, the large variation in lamin A-GFP expression (see also Fig. 1A). Similar data were obtained for the lamin AΔ10 transfected cell line (not shown). It is evident that the lamin A-GFP signal intensity shows a linear correlation with the increase in intensity of the immunostaining with the lamin A antibody (Fig. 2C). Cells transfected with lamin C-GFP did not show any prominent change in immunofluorescence intensity with the lamin A antibody and had a similar distribution to untransfected cells (compare Fig. 2B and D). This also indicates that the incorporation of lamin C-GFP into the nuclear lamina does not interfere with native lamin A expression. Reciprocal experiments using lamin C antibodies combined with lamin A-GFP transfectants were not possible since no lamin C-specific antibodies were available.

Processing of lamin A-GFP and lamin AΔ10-GFP

To examine whether or not lamin A-GFP and lamin AΔ10-GFP were properly processed we used the α-PA antibody that specifically recognizes the carboxy-terminal site of prelamin A (Sinensky et al., 1994a). During (normal) farnesylation-dependent processing this part of prelamin A is cleaved off

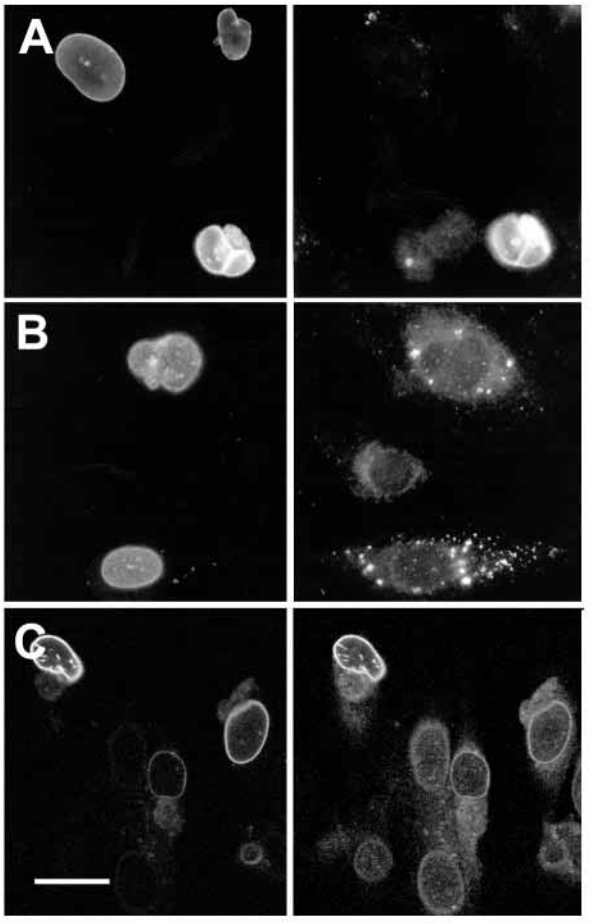

Fig. 3. Processing of lamin A-GFP visualized by immunocytochemical detection of prelamin A. (A) Double fluorescence picture of CHO-K1 cells transfected with lamin A-GFP. Cells with low to moderate levels of GFP fluorescence (left) showed no nuclear prelamin A immunostaining (right). Note, however, that a cell with very high GFP signals also shows anti-prelamin A immunostaining. (B) Double fluorescence picture of lamin AΔ10-GFP fluorescence (left) and prelamin A immunostaining (right). Cells with GFP signal show no nuclear staining with the prelamin A antibody. Several cells do show bright cytoplasmic dots with this antibody (right), indicating that prelamin AΔ10 is present in the cytoplasm and not in the nucleus of these cells. (C) Linear projection of confocal optical sections of lamin A-GFP transfected CHO-K1 cells, treated overnight with 50 μM lovastatin. Left panel, GFP signal. Right panel, immunostaining with the prelamin A antibody. Note that both lamin A-GFP positive and lamin A-GFP negative cells (left) show a nuclear prelamin A signal (right) after treatment with lovastatin. Bar,15 μm (A,B), 20 μm (C).

from the molecule and will be no longer visible with the α-PA antibody. In the lamin A-GFP transfected cultures most cells did indeed show no immunocytochemical staining of prelamin A, suggesting that only processed lamin A-GFP was present in the nucleus. Only in cases of overexpression of lamin A-GFP (as deduced from a very bright GFP signal), could prelamin A be detected in nuclei of these cells (compare left and right panel of Fig. 3A). Similarly, cells transfected with lamin AΔ10-GFP cDNA showed no nuclear staining with the α-PA antibody, indicating also that prelamin AΔ10-GFP is properly processed

(compare left and right panels of Fig. 3B). Unprocessed prelamin AΔ10-GFP was occasionally visible as bright dots in the cytoplasm of some cells (Fig. 3B, right panel).

Cells were treated with lovastatin in order to block the farnesylation step and thus to prevent the processing of prelamins. The α-PA antibody now did show a nuclear immunofluorescence staining in all cells (Fig. 3C, right panel), indicating that the removal of the carboxy-terminal part of prelamin A could indeed be prevented. 3-D analysis of the prelamin A staining showed immunofluorescence staining in intranuclear tubule-like structures, similar to those found in A-type lamin-GFP fluorescence images (see below). The proper processing of lamin A-GFP was confirmed by pulse-chase immunoprecipitation studies with the both the α-PA and lamin A antibody (data not shown).

All three GFP-tagged A-type lamins are present in intra- and transnuclear tube-like structures

More than 50% of the living CHO cells transfected with A-type lamin-GFP constructs revealed, next to lamina fluorescence, intra- and transnuclear tubule-like structures (Fig. 4). Stereo projections of living cells showed that most tubules originate from the surface of the nuclear envelope and extend deep into the nucleus, often traversing the whole nucleus and branching (Fig. 4A-C). Depth viewing of these nuclei also shows that most tubules run from the top to the bottom of the nuclei, i.e. most of them have an orientation vertical to the cell growth surface. Similar intra- and transnuclear tubules could be observed in a low percentage of untransfected CHO-K1 cells after immunostaining with the lamin A antibody (Fig. 4D). However, using the lamin A/C antibodies, these structures were barely visible (not shown). In the majority of untransfected cells, no intranuclear structures other than isolated foci could be detected using conventional immunofluorescence. Immunostaining of A-type lamin-GFP transfected cells with an anti-GFP antibody revealed a staining pattern similar to the immunostaining with the A-type lamin antibodies, and also lacked the recognition of the intranuclear tubules (not shown).

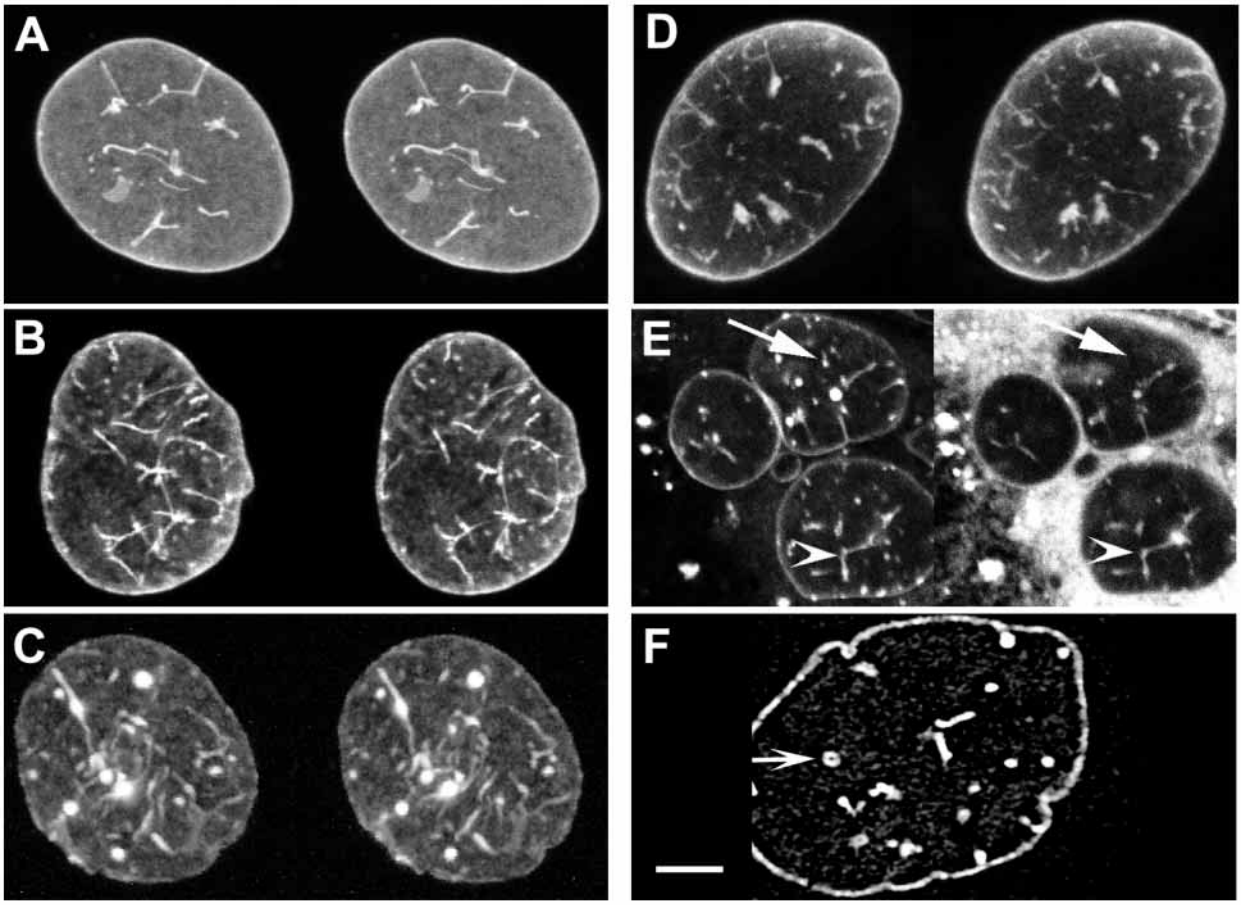

Fig. 4. (A-C) Stereo projections of optical sections obtained by confocal laser microscopy of living CHO-K1 cells. (A) Cells transfected with the lamin A-GFP construct, (B) the lamin AΔ10-GFP construct and (C) the lamin C-GFP construct. Note the prominent fluorescence of intra- and transnuclear tubule-like structures and their branching. (D) Stereo projection of a nucleus of an untransfected CHO-K1 cell stained with the lamin A antibody by indirect immunofluorescence. Note the presence of intranuclear structures similar to those seen in transfected cells. (E) Single slice of a *z*-series of lamin C-GFP transfected cells showing GFP fluorescent intranuclear tubules (left panel), part of which are stained with rhodamine B hexyl ester dye (right panel). Note that several intranuclear structures show both GFP and membrane dye labeling (arrowheads left and right), while other structures do show GFP fluorescence, but no membrane dye staining (arrows). (F) Single optical section of a *z*-series of a lamin A-GFP transfected cell after fixation with formaldehyde. The image was obtained after applying 3-D image restoration software. The arrow indicates a cross-section of a hollow tubule in the nucleus of this cell. Note also the finely speckled interior of this nucleus. Bar, 5 μm (A-D); 10 μm (E); 4 μm (F).

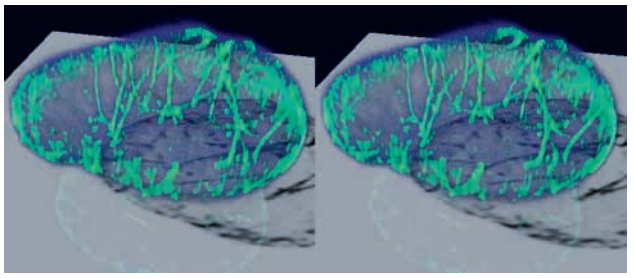

Fig. 5. Volume visualization of restored images from Fig. 4B, using the Simulated Fluorescence Process (SFP) algorithm of the FluVR volume rendering software. The stereoscopic pair was generated by rotating the perspective projected scene over a 2.2° angle around the origin. To improve depth viewing, three different false colors were assigned to different fluorescence intensities, ranging from dark blue (weak signal) to bright green (strong signal). The location of the (fictional) glass slide is shown in grey.

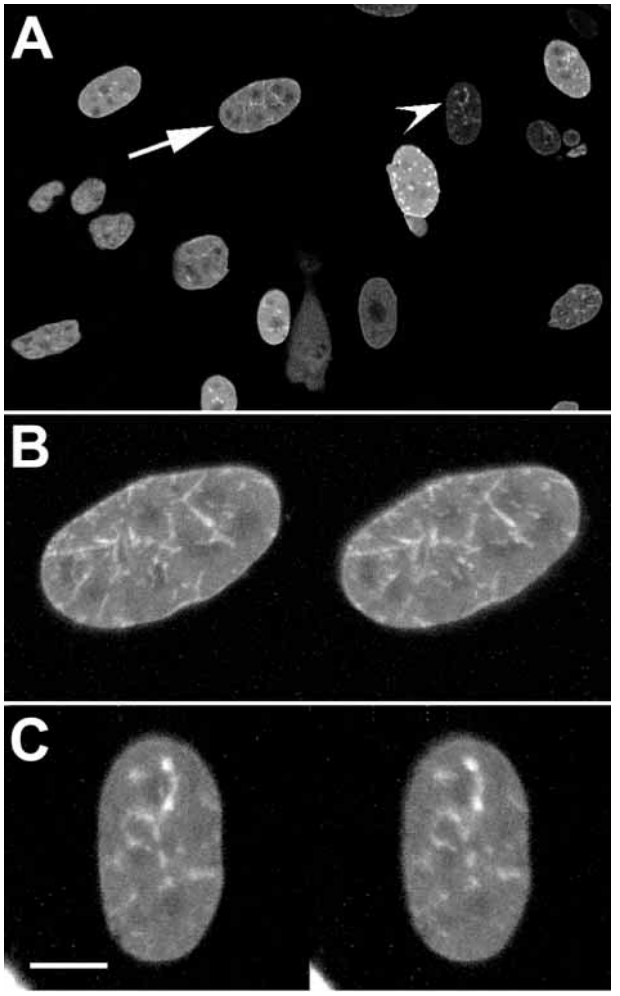

Fig. 6. (A) Overview of a monoclonal culture of CHO-K1 cells after transfection with lamin C-GFP. Note the large heterogeneity in GFP fluorescence levels. (B) Side-by-side stereo projection of a moderately bright fluorescing nucleus (arrow in A). (C) Side-by-side stereo projection of a weakly fluorescing nucleus (arrowhead in A). Bar, 15 μm (A); 5 μm (B); 4 μm (C).

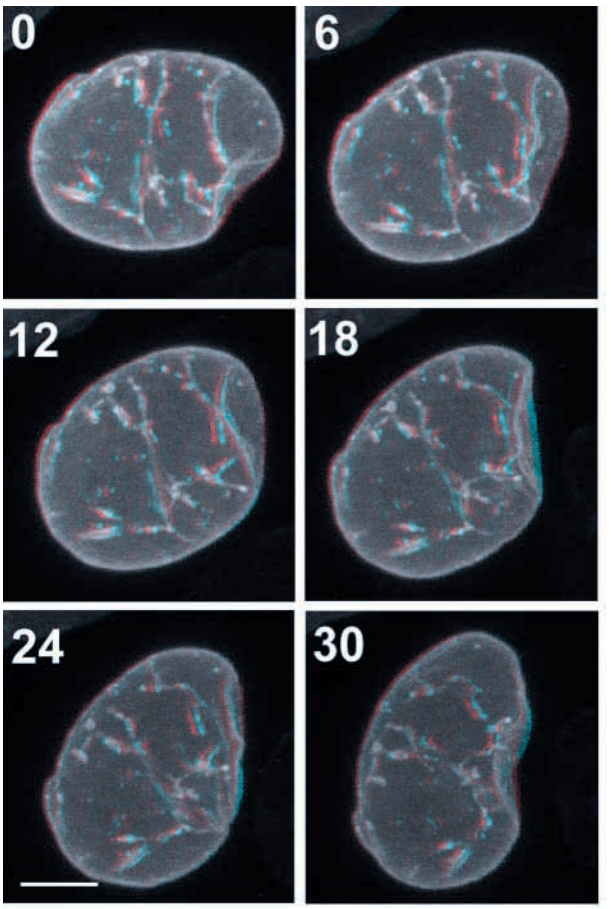

Fig. 7. Selection of 3-D projections of a time-lapse series of a living interphase CHO-K1 cell transfected with lamin C-GFP. The complete recording of this series of images is available as a quicktime and AVI movie at http://137.120.28.214/mcb/cytoskeleton.html#GFP and at www.biologists.com. Over a 30 minute period every minute a 3-D stack of pictures was collected (taking about 15 seconds), and each stack was projected at an angle of 4° to obtain 3-D perception. These images should be viewed with red-green anaglyph glasses. Note the rotation of the nucleus and the extensive folding and local indentation of the nuclear lamina. In contrast, the intranuclear tubules remain stable in appearance and orientation. Bar, 4 μm.

Staining of membrane structures with the rhodamine B hexyl ester dye (R6) (Fig. 4E, right) revealed that some of the intranuclear A-type GFP-lamin structures (Fig. 4E, left) are associated with membrane structures (arrowhead, Fig. 4E), while other intranuclear tubules did not correlate with such a membrane staining (arrow, Fig. 4E). Occasionally, individual optical sections were suggestive of a hollow nature of some of these tubules, both in living cells (not shown) and in fixed cells (Fig. 4F).

The combination of extensive image restoration and a projection method stressing depth view allowed a side-view with enhanced resolution, resulting in a better perception of the organization of the intranuclear tubular structures. A side-view projection of the z-series of the nucleus, shown in Fig. 4B, reveals that most of the intranuclear structures are positioned upright towards the fictional glass slide (Fig. 5).

The presence of intra- and transnuclear tubules was evident

in cells with both high and low lamin-GFP expression levels. Fig. 6A shows an overview of a cell culture of lamin C-GFP transfected CHO-K1 cells. Note the considerable heterogeneity in expression levels of lamin C-GFP. 3-D projection of a *z*-series of a cell with a high level of lamin C-GFP (arrow in Fig. 6A, projection in Fig. 6B) and a cell with a low level of lamin C-GFP expression (arrowhead in Fig. 6A, projection in Fig. 6C) showed that the presence of lamin tubules is independent of the expression level of the chimeric protein.

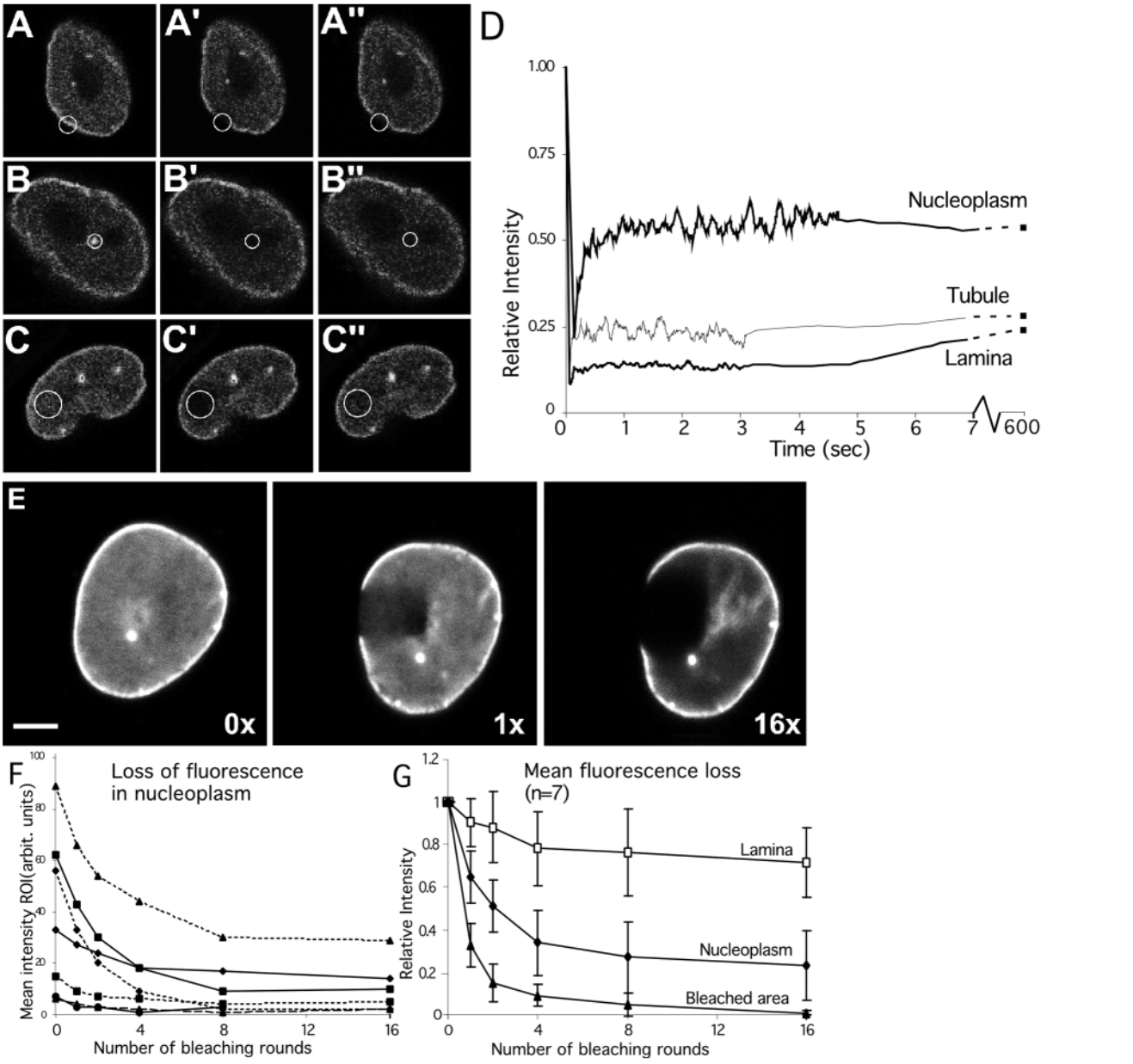

Fig. 8. Fluorescence recovery after bleaching experiments of CHO-K1 cells transfected with lamin C-GFP. Bleached areas are encircled in white. Single slice confocal recordings are shown at T=0 (before bleaching; A-C), immediately after bleaching (T=100 ms; A′-C′), and at 1.5 seconds after bleaching (A″-C″). Bleaching was performed in 3 different areas, i.e. nuclear lamina (A); intranuclear tubule (B); intranuclear area without significant structural characteristics (C). Note that no rapid recovery of GFP signal was observed in either the nuclear lamina or the intranuclear tubules, while in the intranuclear area a restoration of GFP signal was observed within 1.5 seconds. Also, much longer observations (up to 1 hour) did not show any recovery of laminar or tubular GFP signal (not shown). (D) Graphic representation of the first 7 seconds of recovery from bleaching of nuclei in A-C. Note the fast recovery of the nucleoplasm and the low recovery in lamina and tubules, even 10 minutes after photobleaching. (E) Loss of fluorescence intensity after repetitive bleaching in a single nucleus. Note that, while the loss of fluorescence signal was considerably higher in the nucleoplasm than in the lamina, not all of the GFP signal was lost outside the bleached area. (F) Graphic representation of the loss of fluorescence in the nucleoplasm of seven different nuclei. Note the high variation between individuals in the amount of signal lost. (G) Mean fluorescence loss of bleached area, lamina and intranuclear area of seven nuclei with different fluorescence intensities. Note that while the fluorescence in the bleached areas decreased to background levels after eight rounds of bleaching, the lamina and the nucleoplasm outside the bleached area showed a considerable retainment of fluorescent signal. Bar, 6 μm (A-C); 3 μm (E).

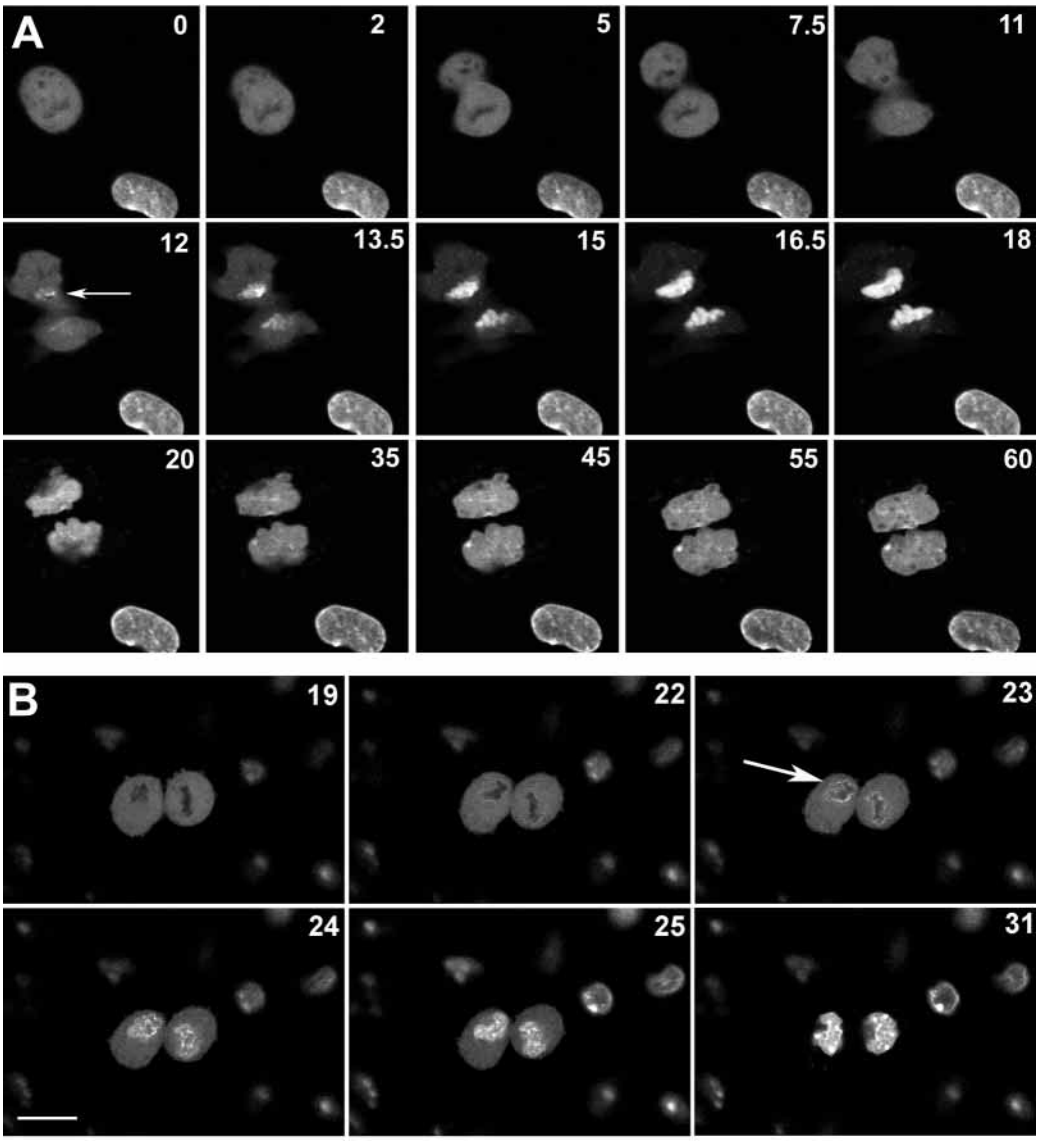

Fig. 9. Time-lapse series of living mitotic CHO-K1 cells transfected with A-type lamins-GFP. Time after start of recordings at metaphase is indicated in minutes in the upper right corner of each picture. Complete recordings are available as quicktime or AVI movies at http://137.120.28.214/mcb/cytoskeleton.html#GFP and at www.biologists.com. (A) Time-lapse series of a mitotic sequence of a lamin A-GFP transfected cell. Note that lamina-like structures did not reoccur until after cytokinesis (arrow). (B) Time-lapse series of a mitotic sequence of a lamin C-GFP transfected cell. Note the reoccurrence of the nuclear lamina after cytokinesis (arrow), and the rapid reoccurrence of brightly fluorescing nuclear dots and prominent intranuclear structures. Bar, 20 μm.

Stability of the lamina and intranuclear tubules in interphase cells

To obtain insight into the dynamics of the intranuclear tubular structures, 3-D imaging over time in selected interphase cells was performed. Fig. 7 shows 3-D projections of an interphase nucleus recorded over a period of 30 minutes. A full-size recording of all images with a 1-minute interval can be observed as a quicktime or AVI movie at Internet site http://137.120.28.214/mcb/cytoskeleton.html#GFP and at www.biologists.com. Our observations indicated that the intranuclear structures were relatively stable, and that their movement followed the horizontal rotation of the nucleus as a whole. They remained vertically oriented towards the glass slide on which they grew and showed no gross alterations in number, shape or relative location within these nuclei. Surprisingly, the nuclear lamina itself seemed more dynamic than the intranuclear tubules, forming indentations and foldings during the time span of 30 minutes. Longer recordings up to 2 hours with time intervals of 15 minutes between each *z*-series confirmed the stability of the intranuclear tubules (data not shown).

A correlation between the intra- and transnuclear structures seen with GFP-tagged lamins and the cell cycle stage was investigated by immunofluorescence staining of PCNA combined with the GFP fluorescence. The tubular lamin structures appeared to be present in both PCNA-positive and PCNA-negative cells, indicating that these structures are present in all interphase stages of the cell cycle (results not

shown). Only when cells entered mitosis did the tubules disappear, along with the nuclear lamina.

Photobleaching

In order to obtain insight into the lateral diffusion of the lamin-GFP chimeras the FRAP technique was applied. Bleaching recovery was very similar for both the lamin C-GFP incorporated into the nuclear lamina (Fig. 8A), and lamin C-GFP present in intranuclear tubules (Fig. 8B). In these areas there was no detectable recovery from photobleaching (Fig. 8A″,B″), and also after 1 hour fluorescence recovery was very low (data not shown). In contrast, lamin C-GFP fluorescence in the nucleoplasm showed a rapid fluorescence recovery within 1.5 seconds after bleaching (Fig. 8C). Quantitiative differences in bleaching recovery of each bleached area are shown in Fig. 8D.

In order to quantify the fraction of freely floating, unbound GFP-lamins in the nucleoplasm, depletion of fluorescence in regions outside the bleached area was measured after repetitive bleaching. Most cells showed that, while there was a considerable loss of fluorescence intensity after repetitive photobleaching, it was impossible to bleach out the intranuclear area completely (Fig. 8E). Choosing both cells with high and with low levels of intranuclear lamin C-GFP expression for these Fluorescence Loss In Photobleaching (FLIP) experiments, it became evident that the variable loss of fluorescence of the nucleoplasm between the individual cells could not be ascribed to differences in the initial fluorescence level of the nucleoplasm (Fig. 8F). The percentage of fluorescence loss ranged in the nucleoplasm between 70% and 100%, with an average loss of 77% (Fig. 8H) after 16 rounds of photobleaching. As expected, the loss of fluorescence in the lamina was much lower (average loss 28%).

A-type lamins reassemble rapidly in a late stage of mitosis

The fate of chimeric lamin-GFP proteins during mitosis was studied by time-lapse analyses of all three lamin-GFP subtypes, starting at metaphase. The full-size recordings of a time series of lamin A-GFP, lamin AΔ10-GFP and lamin C-GFP can be viewed as quicktime or AVI movies at Internet site http://137.120.28.214/mcb/cytoskeleton.html#GFP and at www.biologists.com. A selection of recordings of the lamin A-GFP transfectant, taken at several phases of mitosis, is shown in Fig. 9A. At metaphase the lamina, as well as intranuclear structures, are absent and the GFP signal appears as a diffuse fluorescent signal in the cytoplasm. At the end of mitosis, not until after cytokinesis, aggregation of GFP signal onto the chromatin was observed within 3 minutes. Almost immediately after enclosure of the chromatin by the lamins, as deduced from the GFP signal, intrachromatin structures became apparent, resulting in the reformation of intranuclear tubules. Similar fluorescence patterns were observed with lamin AΔ10-GFP cells or with lamin C-GFP cells (Fig. 9B). In these latter cells a reappearance of the intranuclear dots (absent at metaphase) next to the nuclear lamina and intranuclear tubules was observed.

Immunostaining on fixed transfected cells using the lamin A antibody 133A2 revealed that the timing of reassembly of lamin A-GFP during the different late mitotic stages was consistent with that of the native lamins (not shown). The assembly of GFP-lamins did not lag behind the assembly of endogenous lamins in any of the experiments.

DISCUSSION

Although nuclear lamins have long been recognized as potentially important proteins in maintaining nuclear shape and chromatin organization, there remain many questions regarding their dynamics and their intranuclear organization. We have generated stable transfectants of CHO-K1 cells expressing lamin A-GFP, lamin AΔ10-GFP or lamin C-GFP to address these questions. Observations in these cells showed that chimeric A-type lamin-GFP proteins behave like native A-type lamins in the lamina, as well as in intra- and transnuclear tubules. Using vital imaging techniques we have obtained more insight into the kinetics of the peripheral and intranuclear tubular lamin structures, and were able to study, in living cells, the reassembly dynamics of each individual A-type lamin during mitosis.

Transfected cells appear to encounter no negative effects on growth or survival, since we were able to generate stable transfectants with a growth rate comparable to untransfected CHO-K1 cells (data not shown). Immunoblotting revealed that the fusion proteins had the expected molecular mass and were recognized by antibodies against A-type lamins. The observation that lamin AΔ10-GFP shows a localization pattern indistinguishable from that of lamin A-GFP indicates that this recently discovered variant (Machiels et al., 1996) is a genuine nuclear lamin protein. Lamin-GFP reveals intranuclear structures that are barely visible by immunocytochemistry.

Processing of GFP-tagged A-type lamins and their assembly into the nucleus

The advent of GFP technology provided opportunities to study lamin incorporation in living cells. Since the carboxy terminus of lamin A, and presumably also of lamin AΔ10, is processed (see below), GFP was fused to the amino-terminal site of the A-type lamins. All three chimeric proteins are found at the nuclear periphery of transfected CHO cells. This suggests that the lamin-GFP fusion proteins are properly incorporated into the nuclear lamina. These proteins could not be removed from the nuclei using an extraction with Triton X-100, DNA/RNAse and high-salt treatment, which is further proof that the lamin-GFP proteins are genuine constituents of the nucleoskeleton.

Several molecular mechanisms have been suggested for the association of lamins with the nuclear membrane. B-type lamins and lamin A are farnesylated, which provides them with a hydrophobic anchorage site for the nuclear membrane. Lamin C is not farnesylated, and the mechanism for incorporation of lamin C into the lamina is not known. It has been suggested that for incorporation, lamin C needs to be associated with farnesylated lamin A (Loewinger and McKeon, 1988), or to form heterodimers with B-type lamins (Ye and Worman, 1995). Also, there is evidence that lamin C needs mitosis to occur in order to be built into the lamina (Horton et al., 1992). Pulse-chase and immunostaining of lamin A-GFP and lamin AΔ10-GFP transfected cells with a prelamin A antibody showed that the chimeric proteins undergo processing, similar to native lamin A, including farnesylation and cleavage of the carboxy-terminal part of these proteins (Sasseville and Raymond, 1995;

Sinensky et al., 1994b). Similar to native lamins, processing of GFP-lamins could be blocked by inhibition of farnesylation using lovastatin.

In the case of overexpression of lamin A(Δ10)-GFP, not all molecules seem to be processed and prelamin A-GFP becomes visible both in nuclear membranes and in intranuclear tubules. These findings indicate that processing of prelamin A-GFP is not a prerequisite for its transportation into the nucleus, which is in accord with previous studies on native lamins (Sasseville and Raymond, 1995; Sinensky et al., 1994b). It is conceivable that the intranuclear foci of prelamin A observed by these groups correspond to the intranuclear tubular structures demonstrated in our study.

Contrary to lamin A-GFP and lamin AΔ10-GFP, expression of high levels of lamin C-GFP often resulted in an intranuclear localization of this lamin subtype, displayed as bright GFP dots. Apparently, overexpression of lamin C results in intranuclear aggregates, as previously described by Pugh et al. (1997). This and other microinjection studies suggest that incorporation of lamin C into the lamina of interphase cells is much slower than incorporation of lamin A (Gerace et al., 1984; Horton et al., 1992). The suggestion that incorporation of lamin C into the lamina is independent of lamin A (Pugh et al., 1997) is supported by our finding that high expression levels of lamin C-GFP do not trigger changes in expression levels of lamin A, nor do they interfere with the organization of lamin A. Moreover, in the human cell line GLC-A1, which expresses very low levels of native lamin A, transfection of lamin C-GFP resulted in abundant GFP fluorescence in the nuclear lamina, while the expression of native lamin A remained low (not shown).

All three A-type lamins associate with intra- and transnuclear tubules.

In a majority of transfected cells we observed intra- and transnuclear tubule-like structures. It may be argued that the tubular structures result from overexpression of lamin GFP. Caution for transfection artifacts is indeed justified since the overexpression of lamin proteins and the presence of a biologically incorrect amino-terminal head domain may impair proper functioning of these proteins. However, so far we have no indications for incorrect biological behaviour except for the intranuclear dots in some lamin C-GFP transfectants. The tubular network was seen in most cells, irrespective of the expression levels of lamin-GFP. Moreover, careful (re-)examination of untransfected CHO-K1 cells by routine immunocytochemistry also revealed lamin A tubules in some cells with an IgG antibody, but not with IgM antibodies, indicating antibody penetration problems in intranuclear structures. The presence of intranuclear structures composed of lamins has been described before in fixed or micro-injected cells (Bridger et al., 1993; Fricker et al., 1997; Moir et al., 1994; Pugh et al., 1997; Sasseville and Raymond, 1995). Our approach allowed the study of the assembly of individual A-type lamin-GFP products in living cells, circumventing fixation, inadequate antibody penetration or distortion of cellular structures by microinjection. It could be shown that all three A-type lamins associate with these structures. In addition, we show that several of the tubules do not only cross the nucleus, but also branch. Staining with the membrane dye rhodamine B hexyl ester suggests that some tubules contain membrane lipids. Similar immunocytochemical studies by others, using an antibody to A- and B-type lamins, also indicated that some intranuclear lamin structures corresponded to nuclear (membrane-containing) channels, while others were not associated with membrane labeling (Fricker et al., 1997). The presence of intra- and transnuclear tubules is also in accordance with a recent study by Ellenberg et al. (1997), which showed the presence of nuclear membrane invaginations using lamin B receptor-GFP.

The intranuclear tubules detected with A-type lamin-GFP have been found both in S-phase cells and in non-S-phase cells. These findings corroborate with those of Fricker et al. (1997), who also found no correlation between the presence of intranuclear channels and proliferation. This is contradictory to studies which suggested that intranuclear aggregates, consisting of A-type lamins (and possibly corresponding to the intranuclear tubules observed in our study) were restricted to G_1-phase cells (Bridger et al., 1993), while intranuclear B-type lamin structures were confined to cells of mid- to late S-phase of the cell cycle (Moir et al., 1994).

Stability and orientation of intranuclear tubules indicate a structural support function

The functional role of the intranuclear structures observed with the A-type lamin-GFP constructs remains largely speculative. These structures are relatively stable in localization and number, and recovery of fluorescence after photobleaching is slow, which indicates that within these structures there is a low protein turnover. These findings argue against a recent suggestion that these tubules can rapidly extend to a particular site of the nucleus to release Ca^{2+} (Lui et al., 1998). However, the presence of an additional, more dynamic system of smaller (tubular) structures, not visible at the light microscopy level, cannot be excluded. The vertical orientation of most intranuclear tubules was striking and is in line with a study of Fricker et al. (1997). Based on the orientation of these structures one would be inclined to assign a structural support function to these tubules.

Chimeric GFP molecules can be used to study lamin dynamics at a molecular level

The use of different bleaching techniques permits the study of the molecular organization of lamin molecules in different cellular compartments. Using this technique we were able to confirm the relatively immobile nature of the lamins as part of the nuclear lamina, as well as in the nuclear tubules, which is similar to the findings of Schmidt and Krohne (1995). They showed a very low recovery rate of nuclear lamins after bleaching of micro-injected fluorescent lamins. Note, however, that we confined the rate of recovery studies to well-defined nuclear areas, i.e. the lamina, tubules or an intranuclear area. Strikingly, we found that, while a prominent portion of the intranuclear lamin C-GFP was not bound to any stable structures, up to 30% of the nucleoplasmic lamin C-GFP was bound to immobile internal nuclear molecular structures, possibly representing (part of) the nucleoskeleton. Indications towards the presence of A-type lamins in the nucleoskeleton have been described previously by immunocytochemical staining techniques (Neri et al., 1999), combined with immunoelectron microscopy (Hozák et al., 1995). However, since these papers describe rather harsh extraction methods to

enable antibody penetration into the chromatin area, there was considerable concern about the introduction of artificial structures into this system.

At present it is unclear whether the amount of unassembled GFP-lamins in the nucleoplasm reflects the relative fraction of unassociated native lamins. Based on the finding that the high variation in loss of intranuclear lamin after repetitive photobleaching was not correlated with the initial intranuclear lamin levels (Fig. 8F), we think that the presence of diffuse lamin-GFP is not a result of incomplete incorporation of chimeric lamins only, but reflects a pool of soluble intranuclear A-type lamins next to the immobile fraction.

A-type lamin dynamics during mitosis

Vital imaging showed that after metaphase, lamina reassembly of all three A-type lamins commences after the separation of the cytoplasm of the daughter cells. At that stage the A-type lamins surround the chromatin very rapidly, since within 3 minutes after initiation of lamin-GFP condensation no GFP signal is any longer visible in the cytoplasm surrounding the chromosomes. The majority of all three A-type lamin molecules do not move towards the newly formed nucleus until cytokinesis is completed. These findings correlate well with immunocytochemical studies, which indicate that reassembly of the lamina starts during later stages of telophase and the beginning of cytokinesis, while the bulk of lamins repolymerize into the lamina when the daughter chromosomes decondense (Chaudhary and Courvalin, 1993). Our studies cannot exclude the possibility that part of the lamin molecules have already concentrated at parts of the chromosome surfaces at late anaphase, as suggested previously (Foisner, 1997; Yang et al., 1997a).

In summary, our paper describes the nuclear organization and the dynamics of all three A-type lamins in living cells visualized by GFP. GFP-tagged lamins behave in a similar way to native lamins. All three subtypes incorporate into the nuclear lamina and into the intra- and transnuclear tubular structures, which can be demonstrated in living cells. These tubular structures are very stable in interphase cells, with respect to both localization and composition. Furthermore, the GFP technology enabled an estimation to be made of the fraction of nuclear matrix-bound intranuclear lamins in individual cells. The reassembly studies of A-type lamins during mitosis show that the dynamics of reformation for each of the A-type lamins into the lamina are similar and commence only after the two daughter cells have separated.

The authors thank Drs Y. Raymond, D. Lane, E. B. Lane, G. Krohnse, G. Warren and M. Sinensky for providing antibodies, and Dr F. McKeon for providing the lamin A cDNA. Dr Bert Schutte is acknowledged for assistance in flow cytometric analyses, and Mrs K. van der Kraan for assistance with confocal microscopy. We thank Merck & Co. Inc. for kindly providing lovastatin. Dr Hans van der Voort (Scientific Volume Imaging B.V., Hilversum, the Netherlands) and Silicon Graphics (de Meern, the Netherlands) are acknowledged for performing image restoration analyses.

REFERENCES

Biamonti, G., Giacca, M., Perini, G., Contreas, G., Zentilin, L., Weighardt, F., Guerra, M., Della Valle, G., Saccone, S., Riva, S. et al. (1992). The gene for a novel human lamin maps at a highly transcribed locus of chromosome 19 which replicates at the onset of S-phase. *Mol. Cell. Biol.* **12**, 3499-3506.

Bridger, J. M., Kill, I. R., O'Farrel, M. and Hutchison, C. J. (1993). Internal lamin structures within G_1 nuclei of dermal fibroblasts. *J. Cell Sci.* **104**, 297-306.

Broers, J. L. V., Machiels, B. M., Kuijpers, H. J. H., Smedts, F., van den Kieboom, R., Raymond, Y. and Ramaekers, F. C. S. (1997). A- and B-type lamins are differentially expressed in normal human tissues. *Histochem. Cell Biol.* **107**, 505-517.

Burke, B., Tooze, G. and Warren, G. (1983). A monoclonal antibody which recognises each of the nuclear lamin polypeptides in mammalian cells. *EMBO J.* **2**, 361-367.

Cance, W. G., Chaudhary, N., Worman, H. J., Blobel, G. and Cordon Cardo, C. (1992). Expression of the nuclear lamins in normal and neoplastic human tissues. *J. Exp. Clin. Cancer Res.* **11**, 233-246.

Chalfie, M., Tu, Y., Euskirchen, G., Ward, W. W. and Prasher, D. C. (1994). Green fluorescent protein as a marker for gene expression. *Science* **263**, 802-805.

Chaudhary, N. and Courvalin, J.-C. (1993). Stepwise reassembly of the nuclear envelope at the end of mitosis. *J. Cell Biol.* **122**, 295-306.

Cheng, L., Fu, J., Tsukamoto, A. and Hawley, R. G. (1996). Use of green fluorescent protein variants to monitor gene transfer and expression in mammalian cells. *Nature Biotechnology* **14**, 606-609.

Chiu, W.-L., Niwa, Y., Zeng, W., Hirano, T., Kobayashi, H. and Sheen, J. (1996). Engineered GFP as a vital reporter in plants. *Curr. Biol.* **6**, 325-330.

Cubitt, A. B., Heim, R., Adams, S. R., Boyd, A. E., Gross, L. A. and Tsien, R. Y. (1995). Understanding, improving and using green fluorescent proteins. *Trends Biochem. Sci.* **20**, 448-455.

De Giorgi, F., Brini, M., Bastianutto, C., Marsault, R., Montero, M., Pizzo, P., Rossi, R. and Rizzuto, R. (1996). Targeting aequorin and green fluorescent protein to intracellular organelles. *Gene* **173**, 113-117.

Ellenberg, J., Siggia, E. D., Moreira, J. E., Smith, C., L, Presley, J. F., Worman, H., J and Lippincott-Schwartz, J. (1997). Nuclear membrane dynamics and reassembly in living cells: targeting of an inner nuclear membrane protein in interphase and mitosis. *J. Cell Biol.* **138**, 1193-1206.

Ellis, D. J., Jenkins, H., Whitfield, W. G. and Hutchison, C. J. (1997). GST-lamin fusion proteins act as dominant negative mutants in Xenopus egg extract and reveal the function of the lamina in DNA replication. *J. Cell Sci.* **110**, 2507-2518.

Foisner, R. (1997). Dynamic organisation of intermediate filaments and associated proteins during the cell cycle. *BioEssays* **19**, 297-305.

Fricker, M., Hollinshead, M., White, N. and Vaux, D. (1997). Interphase nuclei of many mammalian cell types contain deep, dynamic, tubular membrane bound invaginations of the nuclear envelope. *J. Cell Biol.* **136**, 531-544.

Furakawa, K., Inagaka, H. and Hotta, Y. (1994). Identification and cloning of an mRNA coding for a germ cell-specific A-type lamin in mice. *Exp. Cell Res.* **212**, 426-430.

Gerace, L. and Burke, B. (1988). Functional organization of the nuclear envelope. *Annu. Rev. Cell Biol.* **4**, 335-374.

Gerace, L., Comeau, C. and Benson, M. (1984). Organization and modulation of nuclear structure. *J. Cell Sci.* **Suppl. 1**, 137-160.

Heim, R., Cubitt, A. B. and Tsien, R. Y. (1995). Improved green fluorescence. *Nature* **373**, 663-664.

Horton, H., McMorrow, I. and Burke, B. (1992). Independent expression and assembly properties of heterologous lamin A and C in murine embryonal carcinoma. *Eur. J. Cell Biol.* **57**, 172-183.

Hozák, P., Sasseville, M.-J., Raymond, Y. and Cook, P. R. (1995). Lamin proteins form an internal nucleoskeleton as well as a peripheral lamina in human cells. *J. Cell Sci.* **108**, 635-644.

Krohne, G. and Benavente, R. (1986). The nuclear lamins. A multigene family of proteins in evolution and differentiation. *Exp. Cell Res.* **162**, 1-10.

Laemmli, U. K. (1970). Cleavage of structural proteins during the assembly of the head of bacteriophage T4. *Nature* **227**, 680-685.

Lin, F. and Worman, H. J. (1993). Structural organization of the human gene encoding nuclear lamin A and nuclear lamin C. *J. Biol. Chem.* **268**, 16321-16326.

Lippincott-Schwartz, J., Presley, J. F., Zaal, K. J. M., Hirschberg, K., Miller, C. D. and Ellenberg, J. (1999). Monitoring the dynamics and mobility of membrane proteins tagged with Green Fluorescent Protein. In *Green Fluorescent Proteins. Methods in Cell Biology*, vol. 58 (ed. K. F. Sullivan and S. A. Kay), pp. 261-281. San Diego: Academic Press.

Loewinger, L. and McKeon, F. (1988). Mutations in the nuclear lamin

proteins resulting in their aberrant assembly in the cytoplasm. *EMBO J.* **7**, 2301-2309.

Ludin, B., Doll, T., Meili, R., Kaech, S. and Matus, A. (1996). Application of novel vectors for GFP-tagging of proteins to study microtubule-associated proteins. *Gene* **173**, 107-111.

Lui, P. P. Y., Kong, S. K., Kwok, T. T. and Lee, C. Y. (1998). The nucleus of HeLa cells contains tubular structures for Ca^{2+} signalling. *Biochem. Biophys. Res. Commun.* **247**, 88-93.

Machiels, B. M., Broers, J. L. V., Raymond, Y., de Ley, L., Kuijpers, H. J. H., Caberg, N. E. H. and Ramaekers, F. C. S. (1995). Abnormal A-type lamin organization in a human lung carcinoma cell line. *Eur. J. Cell Biol.* **67**, 328-335.

Machiels, B. M., Ramaekers, F. C. S., Kuijpers, H. J. H., Groenewoud, J. S., Oosterhuis, J. W. and Looijenga, L. H. J. (1997). Nuclear lamin expression in normal testis and testicular germ cell tumors of adolecents and adults. *J. Pathol.* **182**, 197-204.

Machiels, B. M., Zorenc, A. H. G., Endert, J. M., Kuijpers, H. J. H., van Eys, G. J. J. M., Ramaekers, F. C. S. and Broers, J. L. V. (1996). An alternative splicing product of the lamin A/C gene lacks exon 10. *J. Biol. Chem.* **271**, 9249-9253.

Marshall, J., Molloy, R., Moss, G. W., Howe, J. R. and Hughes, T. E. (1995). The jellyfish green fluorescent protein: a new tool for studying ion channel expression and function. *Neuron* **14**, 211-215.

McKeon, F. D., Kirschner, M. W. and Caput, D. (1986). Homologies in both primary and secondary structure between nuclear envelope and intermediate filament proteins. *Nature* **319**, 463-468.

Moir, R. D., Montag-Lowy, M. and Goldman, R. D. (1994). Dynamic properties of nuclear lamins: lamin B is associated with sites of DNA replication. *J. Cell Biol.* **125**, 1201-1212.

Monosov, E. Z., Wenzel, T. J., Lüers, G. H., Heyman, J. A. and Subramani, S. (1996). Labeling of peroxisomes with green fluorescent protein in living *P. pastoris* cells. *J. Histochem. Cytochem.* **44**, 581-589.

Neri, L. M., Raymond, Y., Giordano, A., Capitani, S. and Martelli, A. M. (1999). Lamin A is part of the internal nucleoskeleton of human erythroleukemia cells. *J. Cell. Physiol.* **178**, 284-295.

Nigg, E. A. (1992). Assembly-disassembly of the nuclear lamina. *Curr. Opin. Cell Biol.* **4**, 105-109.

Ogawa, H., Inouye, S., Tsuji, F. I., Yasuda, K. and Umesono, K. (1995). Localization, trafficking, and temperature-dependence of the *Aequorea* green fluorescent protein in cultured vertebrate cells. *Proc. Natl. Acad. Sci. USA* **92**, 11899-11903.

Olson, K. R., McIntosh, J. R. and Olmsted, J. B. (1995). Analysis of MAP4 function in living cells using green fluorescent protein (GFP) chimeras. *J. Cell Biol.* **130**, 639-650.

Pollard, K. M., Chan, E. K. L., Grant, B. J., Sullivan, K. F., Tan, E. M. and Glass, C. A. (1990). In vitro posttranslational modification of lamin B cloned from a human T-cell line. *Mol. Cell. Biol.* **10**, 2164-2175.

Pugh, G. E., Coates, P. J., Lane, E. B., Raymond, Y. and Quinlan, R. A. (1997). Distinct nuclear assembly pathways for lamins A and C lead to their increase during quiescence in Swiss 3T3 cells. *J. Cell Sci.* **110**, 2483-2493.

Riemer, D., Stuurman, N., Berrios, M., Hunter, C., Fisher, P. A. and Weber, K. (1995). Expression of Drosophila lamin C is developmentally regulated: analogies with vertebrate A-type lamins. *J. Cell Sci.* **108**, 3189-3198.

Rizzuto, R., Brini, M., Pizzo, P., Murgia, M. and Pozzan, T. (1995). Chimeric green fluorescent protein as a tool for visualizing subcellular organelles in living cells. *Curr. Biol.* **5**, 636-642.

Röber, R. A., Weber, K. and Osborn, M. (1989). Differential timing of nuclear lamin A/C expression in the various organs of the mouse embryo and the young animal: a developmental study. *Development* **105**, 365-378.

Sasseville, A. M. J. and Raymond, Y. (1995). Lamin A precursor is localized to intranuclear foci. *J. Cell Sci.* **108**, 273-285.

Schmidt, M. and Krohne, G. (1995). In vivo assembly kinetics of fluorescently labeled Xenopus lamin A mutants. *Eur. J. Cell Biol.* **68**, 345-354.

Schutte, B., Tinnemans, M. M. F. J., Pijpers, G. F. P., Lenders, M. H. J. H. and Ramaekers, F. C. S. (1995). Three parameter flow cytometric analysis: simultaneous detection of cytokeratin, proliferation associated antigens and DNA content. *Cytometry* **21**, 177-186.

Shepp, L. A. and Vardi, Y. (1982). Maximum lilkelihood reconstruction for emission tomography. *IEEE Trans. on Medical Imaging* **MI-1**, 113-121.

Sinensky, M., Fantle, K. and Dalton, M. (1994a). An antibody which specifically recognizes prelamin A but not mature lamin A: application to detection of blocks in farnesylation-dependent protein processing. *Cancer Res.* **54**, 3229-3232.

Sinensky, M., Fantle, K., Trujillo, M., MacLain, T., Kupfer, A. and Dalton, M. (1994b). The processing pathway of prelamin A. *J. Cell Sci.* **107**, 61-67.

Spann, T. P., Moir, R. D., Goldman, A. E., Stick, R. and Goldman, R. D. (1997). Disruption of nuclear lamin organization alters the distribution of replication factors and inhibits DNA synthesis. *J. Cell Biol.* **136**, 1201-1212.

van der Voort, H. T. M., Messerli, J. M., Noordmans, H. J. and Smeulders, A. W. M. (1993). Volume visualization for interactive microscopic analysis. *Bioimaging* **1**, 20-29.

van der Voort, H. T. M. and Strasters, K. C. (1995). Restoration of confocal images for quantitative image analysis. *J. Microsc.* **178**, 165-181.

Verheijen, R., Kuijpers, H. J. H., Schlingeman, R. O., Boehmer, A. L. M., van Driel, R., Brakenhoff, G. J. and Ramaekers, F. C. S. (1989). Ki-67 detects a nuclear matrix-associated proliferation-related antigen. Intracellular localization during interphase. *J. Cell Sci.* **92**, 123-130.

Yang, L., Guan, T. and Gerace, L. (1997a). Integral membrane proteins of the nuclear envelope are dispersed throughout the endoplasmic reticulum during mitosis. *J. Cell Biol.* **137**, 1199-1210.

Yang, L., Guan, T. and Gerace, L. (1997b). Lamin-binding fragment of LAP2 inhibits increase in nuclear volume during the cell cycle and progression into S phase. *J. Cell Biol.* **139**, 1077-1087.

Ye, Q. and Worman, H. J. (1995). Protein-protein interactions between human nuclear lamins expressed in yeast. *Exp. Cell Res.* **219**, 292-298.

Yeh, E., Gustafson, K. and Boulianne, G. L. (1995). Green fluorescent protein as a vital marker and reporter of gene expression in *Drosophila*. *Proc. Natl. Acad. Sci. USA* **92**, 7036-7040.

Zatloukal, K., Denk, H., Spurej, G. and Hutter, H. (1992). Modulation of protein composition of nuclear lamina – reduction of lamins-B1 and lamins-B2 in livers of griseofulvin-treated Mice. *Lab. Invest.* **66**, 589-597.